

## Synthesis, Crystal Structure, and Vibrational Spectroscopy of $K_2Ca_4Si_8O_{21}$ —An Unusual Single-Layer Silicate Containing $Q^2$ and $Q^3$ Units

E. Arroyabe, R. Kaindl, D.M. Töbrens, and V. Kahlenberg\*

*Institute of Mineralogy and Petrography, University of Innsbruck, Innrain 52, A-6020 Innsbruck, Austria*

Received September 4, 2009

Single crystals of the previously unknown potassium calcium silicate  $K_2Ca_4Si_8O_{21}$  (**1**) have been grown from a nonstoichiometric melt as well as using a KCl flux. The compound is triclinic with the following basic crystallographic data: space group  $P\bar{1}$ ,  $a = 6.8052(3)$  Å,  $b = 7.1049(3)$  Å,  $c = 11.2132(5)$  Å,  $\alpha = 96.680(4)^\circ$ ,  $\beta = 105.280(4)^\circ$ ,  $\gamma = 109.259(4)^\circ$ ,  $Z = 1$ ,  $V = 481.28(4)$  Å<sup>3</sup>. The crystal structure was solved by direct methods based on a single-crystal diffraction data set collected at ambient conditions. From a structural point of view,  $K_2Ca_4Si_8O_{21}$  belongs to the group of single-layer silicates. The layers parallel to (001) are characterized by a complex arrangement of 6-, 8-, 10-, and 12-membered tetrahedral rings. The sheets can be built from the condensation of loop-branched *fünfer* single chains running parallel to [100], i.e., the crystallochemical formula can be written as  $K_2Ca_4\{IB,5,1_\infty^2\}[Si_8O_{21}]$ . Compound **1** is the first example of a loop-branched layer silicate containing secondary ( $Q^2$ ) as well as tertiary ( $Q^3$ ) tetrahedra. Linkage between the layers is provided by calcium and potassium cations, which are distributed among a total of three crystallographically independent nontetrahedral sites. Alternatively, the structure can be described as a heteropolyhedral framework, based on  $SiO_4$  tetrahedra and  $CaO_6$  octahedra. The irregularly coordinated K-cations in turn are incorporated in tunnels of the network running parallel to [110]. The structural investigations have been completed by Raman spectroscopy. The allocation of the bands to certain vibrational species has been aided by density functional theory (DFT) calculations.

### Introduction

The application of main group element silicates covers a broad range from construction materials such as Portland cements to inorganic glasses and further on to more sophisticated materials like catalysts and highly selective adsorbents. Furthermore, because silicates are the major constituents of the Earth's crust and mantle, they have been also studied in great detail by geoscientists. Consequently, one should expect that the phase relationships and the crystal structures of this class of compounds are well understood. However, a thorough inspection of the available literature reveals that for many ternary and even binary silicate systems this optimistic assumption does not hold. With this regard the system  $K_2O$ – $CaO$ – $SiO_2$  can serve as a good example. So far the only copious study was performed in 1930.<sup>1</sup> The phase diagram was further completed by a small number of subsequent investigations.<sup>2,3</sup> However, it has to be emphasized that the results concerning the number of existing potassium calcium silicates, their chemical composition, their melting

points and melting behavior, etc., are contradicting. This may be at least partially attributed to the facts that especially in the  $SiO_2$ -rich part of the system (a) equilibrium conditions are notoriously difficult to obtain and (b) samples tend to form glasses upon cooling from the molten state. As an extension of our ongoing research activities on the crystal chemistry of alkali–alkaline earth silicates, we obtained single crystals of the previously unknown compound  $K_2Ca_4Si_8O_{21}$  (denoted as **1**). This article presents the results of X-ray single crystal diffraction and Raman spectroscopic investigations on this material. Moreover, a comparison with other structurally related “diluted” single-layer silicates exhibiting Si:O ratios lower than 1:2.5 is given.

### Experimental Details

**Synthesis.** Single crystals of **1** were grown by two different methods. First, they were obtained in an experiment intended on the production of polycrystalline  $K_2Ca_3Si_6O_{16}$  according to the data given in the phase diagram of Morey, Kracek, and Bowen.<sup>1</sup> Hence, dried  $K_2CO_3$  (AlfaAesar, puratronic),  $CaCO_3$  (AlfaAesar, 99.995%) and  $SiO_2$  (AlfaAesar, 99.995%) in a ratio of 1:3:6 were mixed under ethanol in an agate mortar and afterward pressed into pellets. The educts were subsequently fired in a resistance heated furnace from room-temperature to 935 °C within 24 h, held at the final temperature for five days and finally quenched in air. In contradiction to the reference phase diagram,<sup>1</sup> a first inspection of the pellet under a polarizing microscope revealed it to be partially molten. The product

\*To whom correspondence should be addressed. E-mail: Volker.Kahlenberg@uibk.ac.at. Phone: +43 (0)512 507 5503. Fax: +43 (0)512 507 2926.

(1) Morey, G. W.; Kracek, F. C.; Bowen, N. L. *J. Soc. Glass Technol.* **1930**, *14*, 149.

(2) Morey, G. W.; Kracek, F. C.; Bowen, N. L. *J. Soc. Glass Technol.* **1931**, *15*, 57.

(3) Gunawardane, R. P.; Glasser, F. P. *Z. Anorg. Allg. Chem.* **1975**, *411*, 163.

contained a larger amount of irregularly shaped birefringent crystals of moderate optical quality, embedded in a polycrystalline matrix, which could be identified as **1**. Moreover, we were able to prepare single crystals of **1** via the flux method. Therefore, a homogenized mixture of the above-mentioned educts in the same ratio was decarbonated at 650 °C for 14 h. The product was subsequently mixed with KCl (Merck p.a.), using a nutrient to flux ratio of 1:5. Twenty milligrams of the starting material were filled into a Pt-capsule (3 mm outer diameter), which was crimped and finally sealed by welding. The sample container was heated within 20 h from 100 to 1100 °C, isothermed for 4 h, and finally cooled to 700 °C with 5 °C/h. Analysis of the run product by dint of powder diffraction revealed polycrystalline KCl to be the major constituent. Larger single crystals were mechanically retrieved from the capsule and could be identified by X-ray single-crystal diffraction as wollastonite (CaSiO<sub>3</sub>), KCl as well as **1**, respectively. The chemical composition of single crystals from the first synthesis route was determined with a JEOL JXA-8100 electron microprobe using the wavelength-dispersive analytical mode with a lateral resolution of 1 μm<sup>3</sup> (15 kV, 10 nA). Orthoclase, diopside and quartz were chosen as standards for K, Ca and Si, respectively, with measurement times of 20 s on peaks and 10 s on background of the X-ray lines. The ratio of 1.000(4):2.046(20):3.985(12) for K:Ca:Si resulted in a chemical formula of K<sub>1.997(8)</sub>Ca<sub>4.085(20)</sub>Si<sub>7.958(23)</sub>O<sub>21</sub> (normalized on 21 oxygen atoms) or K<sub>2</sub>Ca<sub>4</sub>Si<sub>8</sub>O<sub>21</sub>.

**Structure Determination.** A transparent, colorless irregularly shaped fragment of relatively good optical quality (0.15 × 0.09 × 0.015 mm in size) was measured on an Oxford Diffraction Gemini R Ultra single crystal diffractometer using graphite-monochromatized MoKα radiation. Intensity data were collected at room-temperature (25 °C) in 320 frames with ω-scans using 1.0° scan width per frame. For integration and data reduction, the CrysAlisPro software package<sup>4</sup> was employed. Semiempirical absorption correction was applied due to the platy habit combined with a linear absorption coefficient of μ = 2.166 mm<sup>-1</sup> for MoKα-radiation. Structure solution and consecutive least-squares refinement calculations were carried out with the programs SIR2004<sup>5</sup> and SHELXL97,<sup>6</sup> respectively, both embedded in the WinGX program suite.<sup>7</sup> Final full matrix least-squares refinement cycles including fractional coordinates and anisotropic displacement parameters for all atoms converged to a residual of R<sub>1</sub> = 0.0278 for 160 parameters and 1736 reflections with I > 2σ(I) (see Table 1). The final difference electron density map was featureless, with maxima and minima of +0.480 and -0.454 e Å<sup>-3</sup>, respectively. Refined atomic coordinates as well as selected interatomic distances are given in Tables 2 and 3. Anisotropic displacement parameters can be found in the CIF file in the Supporting Information. Figures showing structural details were prepared using the program ATOMS.<sup>8</sup> The chemical composition K<sub>2</sub>Ca<sub>4</sub>Si<sub>8</sub>O<sub>21</sub>, derived from the structural investigations is in excellent accordance with the result of the electron microprobe analysis.

**Raman Spectroscopy.** Confocal Raman spectra of a single crystal were obtained with a HORIBA JOBIN YVON Lab-Ram-HR 800 Raman microspectrometer. The sample was excited using the 514.5 nm emission line of a 30 mW Ar<sup>+</sup> laser and an OLYMPUS 100x objective (N.A. = 0.9). Size and power of the laser spot on the surface were approximately 1 μm and 2 mW. The spectral resolution, determined by measuring the Rayleigh line, was about 2 cm<sup>-1</sup>. The dispersed light was

**Table 1.** Data Collection and Refinement Parameters for K<sub>2</sub>Ca<sub>4</sub>Si<sub>8</sub>O<sub>21</sub>

Crystal Data	
<i>a</i> (Å)	6.8052(3)
<i>b</i> (Å)	7.1049(3)
<i>c</i> (Å)	11.2132(5)
α (deg)	96.680(4)
β (deg)	105.280(4)
γ (deg)	109.259(4)
<i>V</i> (Å <sup>3</sup> )	481.28(4)
space group	$P\bar{1}$
<i>Z</i>	1
chemical formula	K <sub>2</sub> Ca <sub>4</sub> Si <sub>8</sub> O <sub>21</sub>
cryst syst	triclinic
density (calcd) (g/cm <sup>-3</sup> )	2.758
absorption coefficient (mm <sup>-1</sup> )	2.166
Intensity Measurements	
index ranges	-8 ≤ <i>h</i> ≤ 6, -7 ≤ <i>k</i> ≤ 9, -14 ≤ <i>l</i> ≤ 14
no. of reflns collected	3987
no. of unique reflns	2026
no. of obsd reflns ( <i>I</i> > 2σ( <i>I</i> ))	1736
<i>R</i> (int) after absorption correction	0.0278
Refinement Parameters	
no. of params	160
final <i>R</i> indices [ <i>I</i> > 2σ( <i>I</i> )]	<i>R</i> <sub>1</sub> = 0.0278, <i>wR</i> <sub>2</sub> = 0.0651
final <i>R</i> indices (all data)	<i>R</i> <sub>1</sub> = 0.0385, <i>wR</i> <sub>2</sub> = 0.0682
GOF on <i>F</i> <sup>2</sup>	1.052

**Table 2.** Atomic Coordinates and Equivalent Isotropic Displacement Parameters (Å<sup>2</sup>) for K<sub>2</sub>Ca<sub>4</sub>Si<sub>8</sub>O<sub>21</sub><sup>a</sup>

	Wyckoff-site	x	y	z	U(eq)
<i>M</i> (1)	2i	0.3360(1)	0.2155(1)	0.1836(1)	0.009(1)
<i>M</i> (2)	2i	0.6316(1)	0.2693(1)	-0.0396(1)	0.009(1)
<i>M</i> (3)	2i	0.2566(1)	0.2912(1)	0.5685(1)	0.019(1)
Si(1)	2i	0.9013(1)	-0.2404(1)	0.1124(1)	0.006(1)
Si(2)	2i	0.8244(1)	0.0983(1)	0.2547(1)	0.006(1)
Si(3)	2i	0.3373(1)	-0.1990(1)	0.5290(1)	0.007(1)
Si(4)	2i	0.1292(1)	-0.4695(1)	0.2582(1)	0.006(1)
O(1)	1f	0.5000	0	0.5000	0.025(1)
O(2)	2i	0.1541(3)	-0.3431(3)	0.3954(2)	0.013(1)
O(3)	2i	0.6119(3)	0.0898(3)	0.1486(2)	0.009(1)
O(4)	2i	0.1230(3)	-0.1250(3)	0.0849(2)	0.012(1)
O(5)	2i	0.3266(3)	0.3103(3)	-0.0018(2)	0.010(1)
O(6)	2i	0.8840(3)	-0.1040(3)	0.2366(2)	0.011(1)
O(7)	2i	0.9138(3)	0.5450(3)	0.1551(2)	0.009(1)
O(8)	2i	0.0495(3)	0.2860(3)	0.2607(2)	0.010(1)
O(9)	2i	0.5327(3)	0.3129(3)	0.3924(2)	0.017(1)
O(10)	2i	0.6561(3)	0.4125(3)	-0.2189(2)	0.011(1)
O(11)	2i	0.8100(3)	0.1185(3)	0.3983(2)	0.011(1)

<sup>a</sup> *M*(1) and *M*(2) represent Ca positions. The *M*(3) site is occupied by K.

collected by a 1024 × 256 open electrode CCD detector. Confocal pinhole was set to 1200 μm. Spectra were recorded unpolarized. Background and Raman bands were fitted by the built-in spectrometer software LabSpec to second order polynomial and convoluted Gauss-Lorentz functions, respectively. Accuracy of Raman line shifts, calibrated by regular measuring the Rayleigh line, was in the order of 0.5 cm<sup>-1</sup>. An observed Raman spectrum of **1** is given in Figure 1.

## Results and Discussion

**Structure.** According to Liebau,<sup>9</sup> **1** belongs to the group of branched single layer silicates. A detailed

(9) Liebau, F. *Structural Chemistry of Silicates: Structure, Bonding and Classification*; Springer-Verlag: Berlin, 1985.

(4) Xcalibur CCD system, CrysAlisPro Software System, Version 1.171.33; Oxford Diffraction Ltd.: Oxford, U.K., 2009.

(5) Farruguaia, L. *J. Appl. Crystallogr.* **1999**, *21*, 837.

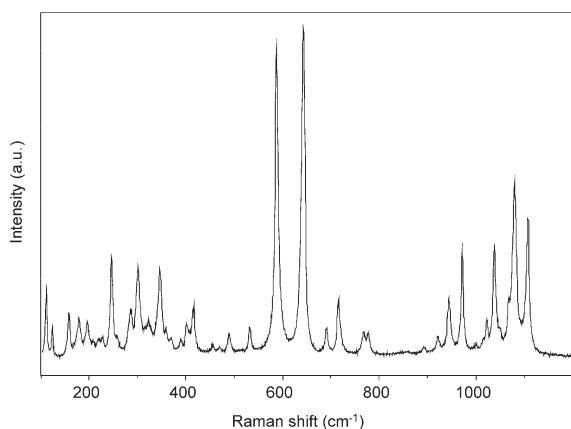
(6) Burla, M. C.; Caliendo, R.; Camalli, M.; Carrozzini, B.; Cascarano, G. L.; De Caro, L.; Giacovazzo, C.; Polidori, G.; Spagna, R. *J. Appl. Crystallogr.* **2005**, *38*, 381.

(7) Sheldrick, G. M. *Acta Crystallogr., Sect. A* **2008**, *64*, 112.

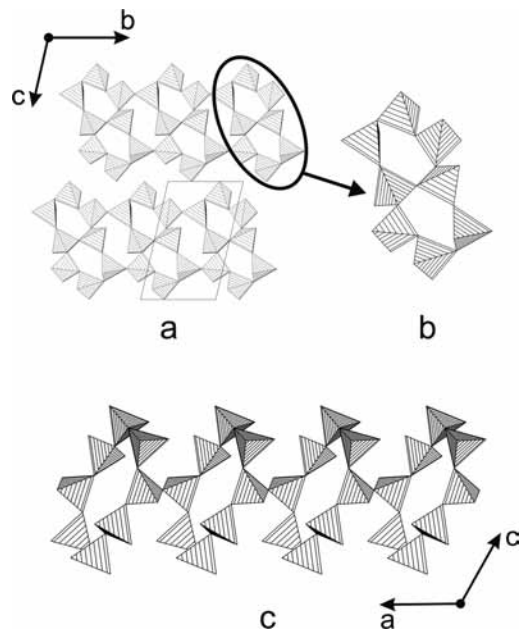
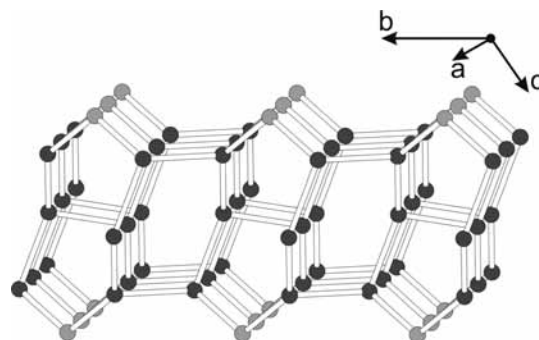
(8) Dowty, E., *ATOMS*, version 5.1; Shape Software: Kingsport, TN, 2000.

**Table 3.** Selected Bond Lengths up to 3.2 Å and Angles (deg)

$M(1)-O(5)$	2.2508 (21)	$M(3)-O9$	2.6235 (22)
$M(1)-O(9)$	2.2616 (21)	$M(3)-O11$	2.8788 (20)
$M(1)-O(4)$	2.3230 (19)	$M(3)-O11$	2.8845 (20)
$M(1)-O(3)$	2.4272 (18)	$M(3)-O10$	2.8949 (20)
$M(1)-O(8)$	2.4965 (19)	$M(3)-O6$	2.8978 (21)
$M(1)-O(10)$	2.6070 (20)	$M(3)-O9$	3.0474 (22)
		$M(3)-O2$	3.0581 (20)
		$M(3)-O1$	3.1900 (7)
$M(2)-O(5)$	2.3254 (19)		
$M(2)-O(4)$	2.3565 (19)		
$M(2)-O(10)$	2.3761 (21)		
$M(2)-O(3)$	2.4838 (19)		
$M(2)-O(7)$	2.5695 (19)		
$M(2)-O(3)$	2.5995 (21)		
$M(2)-O(5)$	2.8746 (19)		
$Si(1)-O5$	1.5887 (19)	$Si(2)-O3$	1.5904 (20)
$Si(1)-O4$	1.5916 (19)	$Si(2)-O6$	1.6222 (19)
$Si(1)-O6$	1.6551 (20)	$Si(2)-O11$	1.6314 (20)
$Si(1)-O7$	1.6717 (20)	$Si(2)-O8$	1.6455 (19)
$Si(3)-O9$	1.5621 (22)	$Si(4)-O10$	1.5759 (19)
$Si(3)-O1$	1.6111 (7)	$Si(4)-O2$	1.6254 (20)
$Si(3)-O2$	1.6325 (21)	$Si(4)-O8$	1.6464 (19)
$Si(3)-O11$	1.6419 (19)	$Si(4)-O7$	1.6522 (19)

**Figure 1.** Unpolarized confocal Raman spectrum of a  $K_2Ca_4Si_8O_{21}$  single crystal.

crystal-chemical classification has been aided by the program CRYSTANA.<sup>10</sup> The resulting crystallochemical formula is  $K_2Ca_4\{IB, 5, 1_{\infty}^2\}[Si_8O_{21}]$ . As shown in Figure 2, the tetrahedral layers parallel to (001) are built up of loop-branched fünfer single chains. One discrete chain has a translation period of about 6.8 Å and runs parallel to [100]. Each single layer contains secondary ( $Q^2$ ) as well as tertiary ( $Q^3$ ) tetrahedra in the ratio of 1:3 inducing in a Si:O-ratio of 2:5.25. Such type of connectivity is exceedingly rare among single layer silicates, which are usually exclusively composed of tertiary tetrahedra.<sup>9</sup> The Si–O distances for the four crystallographically different tetrahedra in the asymmetric unit range from 1.562 to 1.672 Å. As expected, the Si–O<sub>br</sub> bonds are significantly longer than the distances between Si and the nonbridging anions. The O–Si–O angles show a pronounced scatter ranging from 101.9 to 119.1° throughout all present polyhedra. Nevertheless, these values are in the expected range for silicates.<sup>9</sup> A quantitative measure of tetrahedral distortion is given by the quadratic elongation  $\lambda$  and the angle variance  $\sigma^2$ ,<sup>11</sup> respectively. These parameters have values of  $\lambda = 1.006$  and  $\sigma^2 = 26.94$  for Si(1),  $\lambda = 1.008$  and

**Figure 2.** (a) The crystal structure of **1** consists of tetrahedral layers parallel to (001), which are built of (b) condensed loop-branched fünfer single chains (c) running parallel to [100].**Figure 3.** Tetrahedral arrangement of the anion complex: light-gray spheres indicate the  $Q^2$ -connected Si(1) atoms. Dark gray spheres in turn represent tertiary T-atoms Si(2), Si(3), and Si(4), respectively.

$\sigma^2 = 33.74$  for Si(2),  $\lambda = 1.004$  and  $\sigma^2 = 18.26$  for Si(3) as well as  $\lambda = 1.006$  and  $\sigma^2 = 26.19$  for Si(4), respectively. The T–O–T angles range from 124.8 to 180.0°; the latter value can be attributed to O(1), which is located on a special position (inversion center). Within the corrugated sheets, six-, 8-, 10-, and 12-membered tetrahedral rings can be identified. The vertex symbols for the tetrahedral centers are as follows:  $8_1$  (for Si(1)),  $8_1.10_1.6_1$  (for Si(2) and Si(4)) and  $6_1.12_4.12_4$  (for Si(3)), respectively.<sup>12</sup> The arrangement of the different tetrahedra in a single layer is shown in Figure 3.

Charge balance is provided by  $K^+$  and  $Ca^{2+}$  cations, distributed among a total of three different nontetrahedral  $M$  positions.  $M(1)$  is octahedrally coordinated ( $\langle M(1)-O \rangle = 2.394$  Å). For  $M(2)$ , a (6 + 1) fold coordination environment is observed. Focusing on the inner six oxygen ligands ( $\langle M(2)-O \rangle = 2.452$  Å) the coordination polyhedron around  $M(2)$  can be also described as a

(10) Klein, H.-J.; Liebau, F. *J. Solid State Chem.* **2008**, *181*, 2412.(11) Robinson, R.; Gibbs, G. V.; Ribbe, P. H. *Science* **1971**, *172*, 567.(12) Bialek, R. *KRIBER*, version 1.1; ETH-Zürich: Zürich, Switzerland 1995.

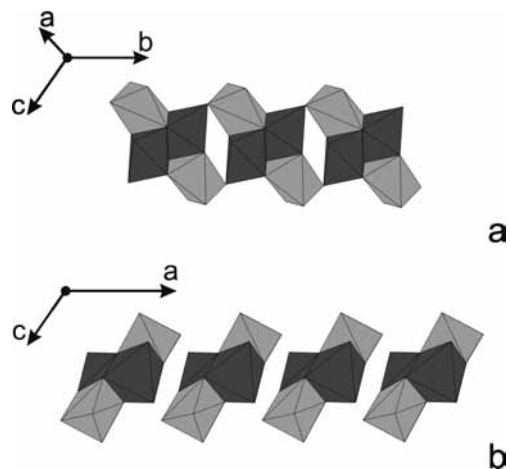


**Figure 4.** (a) Octahedrally arranged cations of **1** form isolated  $[M_4O_{14}]$  bands running along  $[010]$ . (b) The bands themselves are arranged in layers parallel to  $(001)$ . Light-gray spheres represent  $M(1)$  spheres, whereas dark-gray spheres stand for  $M(2)$ .

distorted octahedron. The  $M(3)$  site in turn has eight nearest oxygen neighbors defining a rather irregular polyhedron ( $\langle M(3)-O \rangle = 2.934 \text{ \AA}$ ).

The octahedra around  $M(1)$  and  $M(2)$  are arranged in bands running along  $[010]$  forming  $[M_4O_{14}]$  basic building units (Figure 4(a)). These chains are built of edge sharing  $MO_6$  octahedra, interlinked via common corners. As shown in Figure 4b, the bands themselves are arranged in sheets parallel to  $(001)$ , which in turn interlink the layered silicate anion complexes. Therefore, the structure can be alternatively classified as a mixed polyhedral framework. The 8-fold coordinated  $M(3)$  sites, occupied by potassium are incorporated in tunnels of the network running parallel to  $[110]$  (Figure 5).

Because typical K–O and Ca–O distances average at about 2.76 and 2.33 Å,<sup>13</sup>  $M(1)$  and  $M(2)$  should be preferentially occupied by Ca, whereas  $M(3)$  should correspond to a potassium site. This assumption was corroborated by bond valence sum calculations based on the parameters of Breese and O’Keefe<sup>14,15</sup> for the Ca–O and K–O bonds using the program VaList.<sup>16</sup> The results are in good agreement with the expected values of +2 and +1 v.u.:  $M(1)$ , 2.00 v.u.;  $M(2)$ , 1.78 v.u.;  $M(3)$ , 1.00 v.u.

Vibrational frequencies of **1** have been computed from first principles.  $M(1)$  and  $M(2)$  were modeled as calcium, and  $M(3)$  as potassium. The computations were performed with the program CRYSTAL 06,<sup>17</sup> using Gaussian basis sets. Basis sets for calcium, silicon, and oxygen were taken from the study of Zicovich-Wilson et al.,<sup>18</sup> using the values from grossular for Ca, and from andradite for Si and O used therein.<sup>18</sup> The contractions are 86–511G(21),

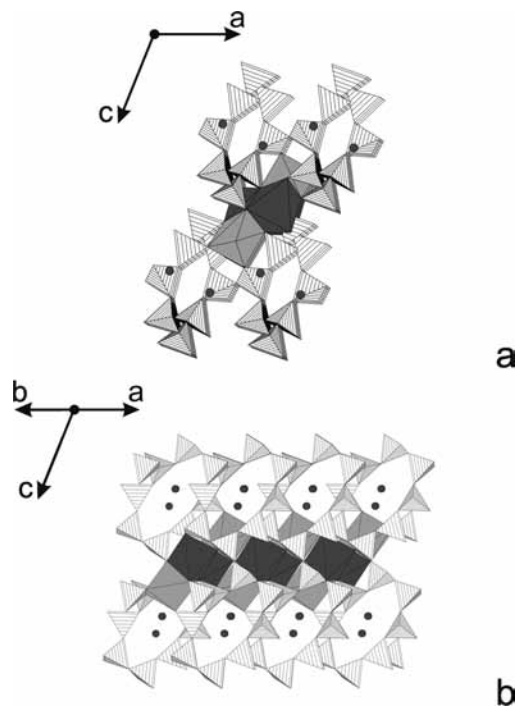


**Figure 5.** (a) Mixed polyhedral framework of **1** seen along  $[010]$ .  $M(1)$  is represented by light-gray octahedra unlike the dark-gray  $M(2)$  spheres. (b) The same extract of the structure seen along  $[110]$  in order to illustrate the incorporation of the 8-fold coordinated K-cations in tunnels of the network running parallel to  $[110]$ .

86–311G(1), 84–11G(1) for Ca, Si, O, respectively. For potassium, the 86–511G(3) basis<sup>19</sup> was adopted. Attempts to further optimize the most diffuse shells did not result in a significant improvement. The full numerical contractions are given in the Supporting Information. The Dirac–Slater (LDA) exchange functional<sup>20</sup> in combination with the Vosko–Wilk–Nusair (VWN) correlation functional<sup>21</sup> was employed. This simple local density approximation was found to give results superior to more sophisticated gradient corrected or hybrid models, both for crystal geometry and Raman line shifts. A Pack–Monkhorst  $k$  net with  $4 \times 4 \times 4$  points in the Brillouin zone was used for the calculations. Modified Broyden damping was applied.<sup>22</sup> The unit cell resulting from this model is uniformly 1% smaller than the experimental unit cell, with negligible anisotropy of the deviation. Because the experimentally determined unit cell was obtained at ambient temperature this deviation is to be expected. The atomic positions of the energetically optimized crystal structure (see the Supporting Information) are very similar to the observed values.

The computational modeling yielded the following irreducible representation of  $K_2Ca_4Si_8O_{21}$  (point group  $I_2$  or  $-1$ ):

$$\Gamma_{\text{vib}} = 51A_g + 54A_u$$

$A_g$  modes are Raman-active,  $A_u$  modes are IR-active. Experimentally, we detected 44 of 51 theoretical

(13) Prince, E. *International Tables for Crystallography, Volume C*; Kluwer Academic Publishers: Dordrecht, The Netherlands, 1995.

(14) Breese, N. E.; O’Keefe, M. *Acta Crystallogr., Sect. B* **1991**, *47*, 192.

(15) Brown, I. D. *The Chemical Bond in Inorganic Chemistry*; Oxford Science Publications: Oxford, U.K., 2002.

(16) Willis, A. S.; Brown, I. *VaList*, version 3.0.15; CEA: Saclay, France, 1999.

(17) Dovesi, R.; Saunders, V. R.; Roetti, C.; Orlando, R.; Zicovich-Wilson, C. M.; Pascale, F.; Civalieri, B.; Doll, K.; Harrison, N. M.; Bush, I. J.; D’Arco, Ph.; Llunell, M. *CRYSTAL06–User’s Manual*; University of Torino: Torino, Italy, 2006.

(18) Zicovich-Wilson, C. M.; Torres, F. J.; Pascale, F.; Valenzano, L.; Orlando, R.; Dovesi, R. *J. Comput. Chem.* **2008**, *29*(13), 2268.

(19) Dovesi, R.; Roetti, C.; Freyria Fava, C.; Prencipe, M.; Saunders, V. R. *Chem. Phys.* **1991**, *156*, 11.

(20) Dirac, P. A. M. *Proc. Cambridge Phil. Soc.* **1930**, *26*, 376.

(21) Vosko, S. H.; Wilk, L.; Nusair, M. *Can. J. Phys.* **1980**, *58*, 1200.

(22) Johnson, D. D. *Phys. Rev B: Condens. Matter* **1988**, *38*, 12807.

**Table 4.** Experimentally Determined Bands, Calculated Frequencies, and Type of Raman-Active Vibrational Modes of  $K_2Ca_4Si_8O_{21}$ <sup>a</sup>

expt	calcd	type	expt	calcd	type
109	115, 118	bs(K–Ca–Si–O),b(K–O)	488	498, 513	bs(Ca–Si–O),b(Ca–Si–O)
121	122, 131	b(K–Si), b(O–K–O)	531	538, 550	sb(Ca–Si–O)
155			587	592	b(O–Si–O)
167	166	bs(K–Ca–Si–O)	641	652	b(O–Si–O)
176	177	s(K–Ca–O)	690	700	s(K–Si–O)
194	190, 198	s(Ca–O), b(Ca–O)	715	721	sb(K–Si–O)
206	209, 210	s(Ca–O)	766	776	bs(K–Si–O)
216			777	792	sb(Ca–Si–O)
224	222	b(O–Ca–O)	891		
244	238, 246	b(O–Ca–O), s(O–Ca–O)	921	929	s(Ca–Si–O)
254	263	b(K–Ca–Si–O)	944	941	s(Si–O)
283	290	bs(Ca–O)	971	980	s(Si–O)
299	299, 308	sb(Ca–O)	999		
320	318, 325	sb(K–Ca–Si–O), s(K–O)	1015	1013	s(Si–O)
344	345	so(K–Si–O)	1022	1022	s(Si–O)
358	351	b(Ca–Si–O)	1038		
367	371	sb(Ca–O)	1045	1042	s(Si–O)
387	382	sb(Ca–Si–O)	1050	1054	s(Si–O)
401	393	b(O–Si–O)	1067	1068	s(Si–O)
413	409	bs(Ca–Si–O)	1079	1085	s(Si–O)
453	458	bs(Ca–K–Si–O)	1103		
468	472	b(K–Si–O)	1107	1112	s(Si–O)

<sup>a</sup> Abbreviations: expt, experimental; calcd, calculated; s, stretching; b, bending; o, other; in brackets, the atoms dominating the specific vibrational mode are given.

observable modes. For a comparison of Raman shifts of observed bands and calculated mode frequencies see Table 4. In general, agreement between observed bands and calculated modes is excellent with maximum deviation of  $15\text{ cm}^{-1}$ . However, in cases where bands can be assigned to more than one vibrational mode, the most probable possibilities are given in Table 4.

In agreement with previous investigations and computational modeling on other alkaline and earth-alkaline silicates,<sup>23,24</sup> bands between  $944\text{--}1107\text{ cm}^{-1}$  are Si–O stretching modes, O–Si–O bending modes dominate around  $401\text{--}641\text{ cm}^{-1}$ , O–Ca–O bending and stretching modes can be found at  $224\text{--}244\text{ cm}^{-1}$ , Ca–O stretching and bending modes at  $194\text{--}299\text{ cm}^{-1}$ , and modes involving mainly potassium at very low frequencies  $< 121\text{ cm}^{-1}$ .

The two strongest bands in the spectrum at 587 and  $641\text{ cm}^{-1}$  are clearly O–Si–O bending modes. A correlation between O–Si–O bond angles and bending mode frequencies was found by quantum chemical calculations on binary sodium silicates.<sup>25</sup> The pronounced scattering of this angle from  $102\text{--}119^\circ$  in **1** is therefore consistent with two O–Si–O bending modes clearly separated by more than 50 wave numbers.

The comparatively large number of bands and frequency ranges of Si–O stretching modes is consistent with the variable Si–O bond lengths (1.562 to 1.672 Å) and the existence of bridging (br)–nonbridging (nbr) oxygens. According to our calculations, four modes can be assigned to Si–O<sub>nbr</sub> bonds (941, 1042, 1054, and  $1085\text{ cm}^{-1}$ ) and another three to Si–O<sub>br</sub> bonds (980, 1068, and  $1112\text{ cm}^{-1}$ ). Two modes at 1013 and  $1022\text{ cm}^{-1}$  involve both Si–O<sub>br</sub> and Si–O<sub>nbr</sub> bonds. This is also in accordance with the results of structure analysis, showing that **1**

is composed of  $[\text{SiO}_4]$  tetrahedra with two and three bridging oxygens ( $Q^2$  and  $Q^3$  units).

**Discussion.** Most of the known single-layer silicates are exclusively built of tertiary ( $Q^3$ )  $\text{SiO}_4$ -tetrahedra, showing a Si:O ratio of 2:5. However, for both cases, namely, increased and reduced connectivities, examples can be found in the literature. The occurrence of monophyllosilicates with quaternary ( $Q^4$ ) and tertiary  $[\text{SiO}_4]$ -tetrahedra has been documented, for example, for  $\text{Na}_2[\text{Si}_3\text{O}_7]$ ,<sup>26</sup>  $\text{Li}_2[\text{Si}_3\text{O}_7]$ ,<sup>27</sup>  $\text{CsH}[\text{Si}_3\text{O}_7]$ ,<sup>28</sup>  $\text{Na}_6[\text{Si}_8\text{O}_{19}]$ ,<sup>29</sup> or  $\text{K}_2[\text{Si}_4\text{O}_9]$ .<sup>30</sup> On the other hand, to the best of our knowledge, only three single-layer silicates, which are composed of  $Q^2$  as well as  $Q^3$  units, have been characterized up to now:

$\text{Na}_2\text{Zn}[\text{Si}_3\text{O}_8]$ <sup>31</sup> belongs to the group of unbranched single-layer silicates. According to the crystal chemical classification of Liebau,<sup>9</sup> the fundamental building blocks of the sheets are unbranched dreier single chains. Each layer is characterized by secondary as well as ternary  $[\text{SiO}_4]$  tetrahedra occurring at a ratio of 1:2 with a resulting Si:O ratio of 2:5.33. By contrast,  $\text{Rb}_6(\text{InCo})_2\text{--}[\text{Si}_9\text{O}_{26}]$ <sup>32</sup> and  $\text{K}_9\text{F}_2\text{Eu}_3[\text{Si}_{12}\text{O}_{32}]$ ,<sup>33</sup> both can be allocated to the group of branched single layer silicates. The rubidium-rich compound is composed of open-branched sechser single chains showing ratios of  $Q^2:Q^3 = 7:2$  and Si:O = 2:5.78, respectively.  $\text{K}_9\text{F}_2\text{Eu}_3[\text{Si}_{12}\text{O}_{32}]$  in turn is made up of open-branched fünfer single chains exhibiting

(26) Kahlenberg, V.; Marler, B.; Munoz Acevedo, J. C.; Patarin *J. Solid State Sci.* **2002**, *4*, 1285.

(27) Krueger, H.; Kahlenberg, V.; Kaindl, R. *J. Solid State Chem.* **2007**, *180*(3), 922.

(28) Wang, X.; Liu, L.; Huang, J.; Jacobson, A. J. *J. Solid State Chem.* **2004**, *177*, 2499.

(29) Krueger, H.; Kahlenberg, V.; Kaindl, R. *Solid State Sci.* **2005**, *7*, 1390.

(30) Swanson, D. K.; Prewitt, C. T. *Am. Mineral.* **1983**, *68*, 581.

(31) Hesse, K.-F.; Liebau, F.; Böhm, H. *Acta Crystallogr., Sect. B* **1977**, *33*, 1333.

(32) Hung, L.-I.; Wang, S.-L.; Chen, Y.-H.; Lii, K.-H. *Inorg. Chem.* **2006**, *45*, 2100.

(33) Tang, M.-F.; Chiang, P.-Y.; Su, Y.-H.; Jung, Y.-C.; Hou, G.-Y.; Chang, B.-C.; Lii, K.-H. *Inorg. Chem.* **2008**, *47*, 8985.

(23) Arroyabe, E.; Kaindl, R.; Kahlenberg, V. *Z. Anorg. Allg. Chem.* **2009**, *635*, 337.

(24) Kahlenberg, V.; Kaindl, R.; Sartory, B. *Solid State Sci.* **2007**, *9*, 65.

(25) You, J.-L.; Jiang, G.-C.; Hou, H.-Y.; Chen, H.; Wu, Y.-Q.; Xu, K.-D. *J. Raman Spectrosc.* **2005**, *36*, 237.

ratios of  $Q^2:Q^3 = 1:2$  and  $Si:O = 2:5.3$ . Like the last two compounds, **1** belongs also to the group of branched single-layer silicates containing  $Q^2$  as well as  $Q^3$  units. However,  $K_2Ca_4Si_8O_{21}$  is the first example of a silicate based on loop-branched chains.

It is interesting to note that silicate structures containing  $[Si_8O_{21}]^{10-}$  anion complexes have been already described in the literature. For example,  $K_4(NbO)_2[Si_8O_{21}]^{34}$  consists of condensed double bands where every single band is built of loop-branched dreier single chains. The compound shows the same Si:O ratio as **1** and both parts of the double-bands contain in each case one  $Q^2$  and three  $Q^3$  tetrahedra. In spite of such explicit structural affinity, the compound is no layer-silicate. A further example is  $K_4In_2[Si_8O_{21}]^{35}$  which consists of  $Q^2$  and  $Q^3$  tetrahedra forming an interrupted framework.

Up to now, no pure natural K–Ca-silicate has been described. However, there are several hydrated potassium calcium silicates with layered structures, such as shlykovite ( $KCa[Si_4O_9(OH)] \times 3 H_2O$ ), cryptophyllite

( $K_2Ca[Si_4O_{10}] \times 5 H_2O$ ) (private communication) or apophyllite ( $KCa_4[Si_8O_{20}(F,OH)] \times 8 H_2O$ )<sup>36</sup> whose sheets are formed by 4- and 8-membered tetrahedral rings. Rhodesite ( $KHCa_2[Si_8O_{19}] \times 5 H_2O$ )<sup>37</sup> is also structurally related with **1**; its layers can be described via the condensation of four-membered rings. However, the hydrous mineral counterparts of **1** are exclusively based on  $Q^3$  tetrahedra.

Finally, we would like to point out that  $K_2Ca_4Si_8O_{21}$  has not been mentioned in the phase equilibrium studies of Morey, Kracek, and Bowen<sup>1</sup> on the ternary system  $K_2O$ – $CaO$ – $SiO_2$ . However, because the composition of the crystalline phases obtained in this early investigation was estimated from the starting composition of the glasses or from the initial weight fractions of the educts it is not unlikely that the postulated phase  $K_2Ca_2Si_9O_{21}$  actually corresponds to **1**, and that  $K_2Ca_4Si_8O_{21}$  represents the correct chemical composition of this potassium calcium silicate.

**Acknowledgment.** The authors thank one of the reviewers for pointing out the existence of the two recently discovered but yet unpublished hydrous K–Ca silicate minerals cryptophyllite and shlykovite.

**Supporting Information Available:** Crystallographic information in CIF format. This material is available free of charge via the Internet at <http://pubs.acs.org>.

(34) Rastsvetaeva, R. K.; Bolotina, N. B.; Pushcharovsky, D.Yu.; Stefanovich, S.Yu.; Nadezhina, T. N.; Dimitrova, O. V. *Kristallografiya* **1994**, 39(6), 1001.

(35) Hung, L.-I.; Wang, S.-L.; Kao, H.-M.; Lii, K.-H. *Inorg. Chem.* **2007**, 46, 3301.

(36) Stahl, K.; Kvik, A.; Ghose, S. *Acta Crystallogr. Sect. B* **1987**, 43, 517.

(37) Hesse, K. F.; Liebau, F.; Merlino, S. Z. *Kristallogr.* **1992**, 199, 25.